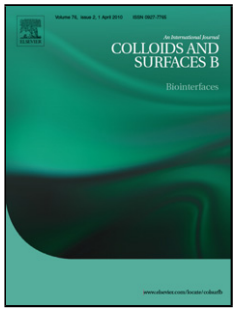

Title: Aptamer@Au-*o*-phenylenediamine modified pencil graphite electrode: A new selective electrochemical impedance biosensor for the determination of insulin

Authors: Ali A. Ensafi, Elaheh Khoddami, B. Rezaei

PII: S0927-7765(17)30499-X
DOI: http://dx.doi.org/doi:10.1016/j.colsurfb.2017.07.076
Reference: COLSUB 8739

To appear in: *Colloids and Surfaces B: Biointerfaces*

Received date: 19-4-2017
Revised date: 21-7-2017
Accepted date: 26-7-2017

Please cite this article as: Ali A.Ensafi, Elaheh Khoddami, B.Rezaei, Aptamer@Au-o-phenylenediamine modified pencil graphite electrode: A new selective electrochemical impedance biosensor for the determination of insulin, Colloids and Surfaces B: Biointerfaceshttp://dx.doi.org/10.1016/j.colsurfb.2017.07.076

Aptamer@Au-*o*-phenylenediamine modified pencil graphite electrode: A new selective electrochemical impedance biosensor for the determination of insulin

Ali A. Ensafi*, Elaheh Khoddami, B. Rezaei

Department of Chemistry, Isfahan University of Technology, Isfahan 84156–83111, Iran

* Corresponding author: Fax: +98–31–33912350; Tel.: +98–31–33912351. E–mail: Ensafi@cc.iut.ac.ir; aaensafi@gmail.com; ensafi@yahoo.com

Graphical abstract

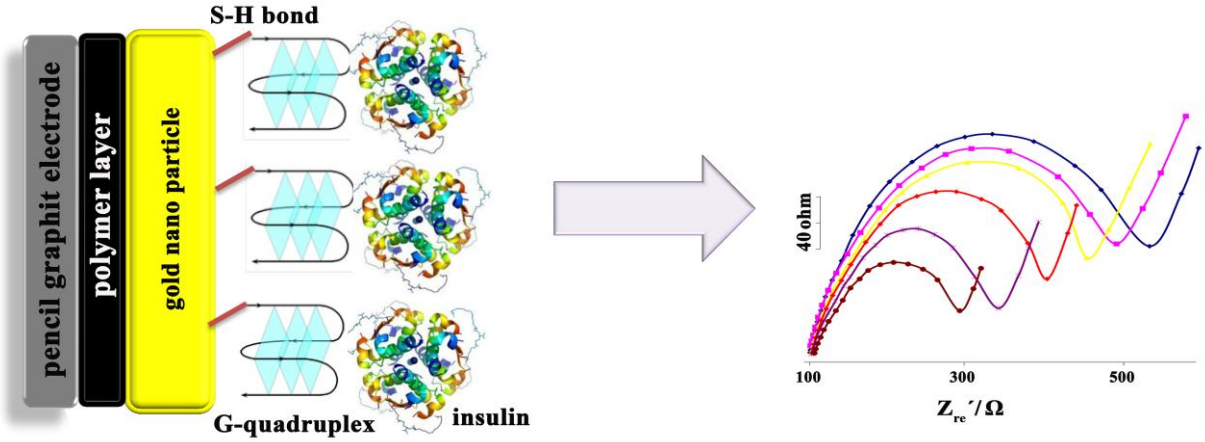

Highlights

- An electrochemical DNA-based biosensor was introduced for insulin.
- Polymer film-gold nanoparticles were used to prepare modified graphite electrode.
- The biosensor could detect insulin as low as 0.027 nmol L^{-1}.
- The efficiency of the biosensor was determined in real urine and plasma samples.

Abstract

In this work, a poly-orthophenylene diamine substrate is decorated with gold nanoparticles (GNPs) and then with single-stranded DNA (ss-DNA) aptamer immobilized on the surface of a pencil graphite electrode (PGE) for the detection and determination of plasma insulin. In this procedure, a polymer layer is formed on the surface of the graphite electrode using anodic oxidation of orthophenylene diamine monomers. The parameters affecting the biosensor sensitivity including the potential applied to form the polymer layer, incubation time, concentration of immobilized ss-DNA, and the presence of $MgCl_2$ (as salt) are evaluated. Electrochemical impedance spectroscopy and cyclic voltammetry are then used to characterize the biosensor. The biosensor is employed under optimal conditions to obtain figures of merit, which reveal a linear range and a limit of detection of 1.0 – 1000.0 nmol L^{-1} and 0.27 nmol L^{-1}, respectively. Finally, the aptasensor is employed for the determination of insulin in real plasma and urine samples to verify its performance and effectiveness.

Keywords: ssDNA aptamer, Insulin, Poly-orthophenylene diamine, Gold nanoparticles, Electrochemical impedance spectroscopy.

1. Introduction

Aptamers have proved excellent sensing systems for the determination of target molecules [1]. A single-stranded DNA/RNA, including 15 – 40 bases with a sequence of A, U/T, C, and G nucleotides, is known as an aptamer which is selected and isolated from a synthetic library via a technology known as “SELEX” (systematic evolution of ligands by exponential enrichment) [2]. Such properties as cost-effectiveness and small size combined with good flexibility and simplicity in designing their determined structure

make them excellent for use as detectors. Modification at the terminal end of the aptamer sequence has been accomplished using combinatorial chemical synthesis methods. Reversibility under thermal denaturation, bioactivity maintenance under harsh conditions, and chemical stability under buffer conditions are also included in the wide range of advantageous aptamer properties [3].

One limitation with aptamer application, however, is its sensitivity to nucleases that are abundant in biological fluids. This has been remedied by applying a specific chemical modification in its synthesis to provide better protection and to enhance its stability [4]. A description of the use of nanoscale biosensors based on aptamers has been provided by Lee et al. [5]. The authors also outlined the advantages of aptamers over antibodies and other detecting elements traditionally used, especially in electrical sensors, and reiterated the high throughput detection of target molecules as a special characteristic of these novel detecting elements.

The single-strand DNA aptamer has been used in extraction studies because of its high selectivity and extraction recovery. Solid-phase extraction (SPE) methods with aptamers have also been reported for target extraction [6,7]. In one study, an aptamer immobilized on beads was employed for the purification of human plasma-related proteins from multiple sources [8]. The same method was also used for purification and immobilization of enzyme from cell lysates for biocatalysis [9]. Extraction based on aptamers (e.g., RNA and DNA or their bio-stables) has also been reported for the separation of a series of enantiomers [10–12].

Conductive polymers have been used in such varied fields as supercapacitors [13] electrochromic devices [14], batteries [15], and biosensors [6,16,17]. Conductive polymer films, which are electropolymerized on the surface of biosensors, are great materials for enhancing biosensor surface area. Regarding the immobilization of biological materials on

the surface of an electrode, these polymers offer such interesting properties as (1) controlling film thickness and homogeneity, (2) improving the mechanical and chemical stability of the films; and (3) enhancing biosensor surface area [17]. Conducting polymers have been widely used in bioanalytical applications, especially in biosensors, owing to their inherent charge transfer properties and biocompatibility [18]. Biosensors with conducting polymers are most commonly used in electrochemical impedance spectroscopy detection [19,20]. Poly-orthophenylene diamine has been considered as a promising conducting polymer owing to its well-defined structure and remarkable stability and conductivity [21,22].

Insulin is a peptide hormone, has a considerable role in regulation of fat and carbohydrate metabolism. The level of insulin is the most critical indicator of the function of endocrine beta cells [23]. Detection of trace amounts of insulin is important in the diagnosis of diabetes and trauma [24].

Recently, Verdian-Doghaei and Housaindokht [25] has been studied the interaction of insulin with a specific aptamer using spectroscopic method. The interaction between a recently developed 30-base-long insulin-binding aptamer and insulin is studied in this paper. The CD spectrum of this aptamer showed a four stranded, parallel G-quadruplex conformation. The spectral characteristics showed that insulin binds to the insulin binding aptamer and promotes the formation of stable G-tetrad structure. This conformational change can be used as a homogeneous aptasensor, molecular aptamer beacon, for insulin detection.

In this study, poly-orthophenylene diamine substrate, as a conductive polymer, equipped with gold nanoparticles (GNPs) single-strand DNA (ss-DNA) aptamer was fabricated at a pencil graphite electrode (PGE). In this study, a 30-base-long insulin-binding aptamer was selected. The anodic oxidation method was used to form the polymer

layer on the surface of PGE using orthophenylene diamine monomers. The biosensor thus produced was used for determination of insulin using electrochemical impedance spectroscopy and cyclic voltammetry. It exhibited a good sensitivity to insulin quantities as low as 0.027 nmol L^{-1}. Finally, the biosensor was used for the determination of insulin in real plasma and urine samples with satisfactory results.

2. Experimental

2.1. Reagents

Orthophenylenediamine and gold(III) chloride trihydrate ($HAuCl_4.3H_2O$) were purchased from Merck (Germany). Deionized water was used throughout the experiments. A 30 mer single-stranded DNA modified with HS-$(CH_2)_6$ at the 5'end was purchased from Takapouzist Company (Iran). The DNA had a sequence of oligonucleotides as 5`-GGT GGT GGG GGG GGT TGG TAG GGT GTC TTC-3`. A stock solution (100 μmol L^{-1}) of the DNA sequences was prepared in sterile distilled water (SD water) and stored in a refrigerator at –20 °C. Subsequently, 100 mL of the acetate buffer was prepared with 2.9 mL of acetic acid and 0.12 g of NaCl. The pH of this solution was adjusted to 5.2 by adding 0.1 mol L^{-1} NaOH solution. Dithiothreitol solution was prepared by dissolving 0.077 g of dithiothreitol in 1.0 mL of the acetate buffer. Sodium dihydrogen phosphate and disodium monohydrogen phosphate (0.1 mol L^{-1}) were used for the preparation of phosphate buffer solutions (PBS) with pH levels ranging from 4.0 to 8.0, and the solution pH was adjusted by adding 0.1 mol L^{-1} of H_3PO_4 or 0.1 mol L^{-1} NaOH to the above mixture. $K_3Fe(CN)_6$ and $K_4Fe(CN)_6$ were obtained from Merck. HB pencil graphite rods (0.7×90 mm, Pentel) were prepared from Japan.

2.2. Apparatus

Electrochemical measurements were performed in an analytical system (Ivium potentiostat/galvanostat, Vertex, Netherlands) linked to a computer using an Ivium 2.231 software that connected to a three-electrode cell including Ag/AgCl (3.0 mol L^{-1} KCl) as a reference electrode, a platinum wire as an auxiliary electrode and a PGE (Pentel, 0.7 mm diameter) modified with GNPs-ss DNA as a working electrode. These electrodes were inserted in a probe solution containing 1.0 mmol L^{-1} $K_3Fe(CN)_6/K_4Fe(CN)_6$ in 0.1 mol L^{-1} KNO_3.

2.3. Method development

In this work, ss-DNA aptasensor was used as a specific device to extract and determine insulin from real samples. PGE was initially activated in a 5 mL solution containing 0.1 mol L^{-1} sodium carbonate and lithium perchlorate in a potential range of −0.40 to +2.00 V at a scan rate of 50 mV s^{-1} using five continuous runs of cyclic voltammetry [26]. The activated electrode was then coated with poly-*o*-phenylene diamine using three continuous cyclic voltammetry responses in 10 mmol L^{-1} of *o*-phenylene diamine (in 0.1 mol L^{-1} potassium chloride) in a potential range of −0.30 to +1.10 V at a scan rate of 25 mV s^{-1}. The surface of the polymer was subsequently coated with gold nanoparticles in 0.003 mol L^{-1} of gold(III) chloride containing 0.1 mol L^{-1} potassium nitrate, in the potential range of –0.50 to +1.50 V at a scan rate of 2 mV s^{-1}. The excess gold ions, trapped on the electrode surface, were removed in the potential range of –0.50 to +1.50 V at a scan rate of 50 mV s^{-1} using ten continuous cyclic voltammetry responses in 0.1 mol L^{-1} potassium nitrate. This layer was modified with the ssDNA using self-assembled S-H group at the end of the ssDNA. For this purpose, the sensor was placed in 200 µL of 15.0 µmol L^{-1} thiolated single-stranded DNA at 3–4 ^{o}C for 90 min. The charge transfer resistance of this aptasensor was evaluated using electrochemical impedance

spectroscopy in 1.0 mmol L^{-1} $K_3Fe(CN)_6/K_4Fe(CN)_6$ solution containing 0.1 mol L^{-1} KNO_3. Insulin was extracted from the sample solution and interacted with the single-stranded DNA to form a G-quadruplex structure at pH 7.4 (containing 10 mmol L^{-1} $MgCl_2$) for 90 min at 20 ^oC. The charge transfer resistance of the aptasensor, after its interaction with insulin, was evaluated using electrochemical impedance spectroscopy in 1.0 mmol L^{-1} $K_3Fe(CN)_6/K_4Fe(CN)_6$ solution containing 0.1 mol L^{-1} KNO_3. The difference in the charge transfers of the biosensor before and after interaction with insulin was used as an analytical signal. The calibration curve was obtained under optimum conditions for insulin detection. A schematic diagram of the fabrication of the biosensor is shown in graphical abstract.

3. Results and discussion

3.1. Electrochemical investigation of the ssDNA aptasensor

The biosensor platform was prepared in several steps. At first, a pencil graphite electrode surface was activated using cyclic voltammetry as explain in Sec. 2.3. Figs. 1A-a and 1A-b show the cyclic voltammograms of the PGEs in 1.0 mmol L^{-1} $K_3Fe(CN)_6/K_4Fe(CN)_6$ solution (containing 0.1 mol L^{-1} KNO_3) before and after electrochemical treatment, respectively. As shown in Fig. 1A-b, the activity of the pretreated PGE is higher than the untreated one. Then, the polymer film was electrodeposited on the surface of the activated PGE in the potential range of –0.30 to +1.10 V in 5 mL of 10.0 mmol L^{-1} orthophenylene diamine and 0.1 mol L^{-1} potassium chloride. Fig. 1A-c shows the cyclic voltammogram of the polymer film modified-activated PGE in the $K_3Fe(CN)_6/K_4Fe(CN)_6$ solution, confirmed that the conductive polymer film is formed at the electrode surface. Afterwards, gold nanoparticles were coated on the polymer film surface in the potential range of –0.50 to +1.50 V at a scan rate

of 2 mV s^{-1}. Increasing in the current of the gold modified electrode (Fig. 1A-d) confirmed the modification. Finally, the ssDNA was self-assembled on the PGE modified with gold nanoparticles decorated on the polymer film. Decreasing the peak current of the modified electrode confirms the success assembling of the ssDNA at the gold-modified electrode (Fig. 1A-e). **"Here Fig. 1"**

Electropolymerization of orthophenylene diamine at the surface of the activated graphite pencil electrode was studied based on the difference between the numbers of cyclic voltammetry. The activated PGE was placed in the probe solution and the current was obtained according to the above procedure and named as I_1. Several cycling were applied for the electropolymerization using a scan rate of 25 mV s^{-1} for voltammogram cycles between 1 to 5 in 5 mL of 10 mmol L^{-1} orthophenylene diamine (containing 0.1 mol L^{-1} KCl). The gold nanoparticles were then coated on the polymer substrate surface in a potential range of –0.50 to +1.50 V as described above. The excess gold ions trapped on the electrode surface were removed in the potential range of –0.50 to +1.50 V at a scan rate of 50 mV s^{-1} using ten CVs in 0.1 mol L^{-1} potassium nitrate solution. The current of the probe solution was then obtained on the surface of the electrode coated with gold nanoparticles (I_2). The difference between these two currents ($\Delta I = I_2 - I_1$) was reported as the result. Based on the results obtained, complete polymerization was achieved with three CVs. It was observed that higher cycle numbers created a thick polymer film that increased the charge transfer resistance which, in turn, affected gold nanoparticle deposition. The polymer layer formed at a small number of CVs was not homogenous and reduced the polymer support for the electrodeposition of gold nanoparticles. Coating of the the polymer layer with gold nanoparticles led to the enhanced electrochemical activity of the electrode because the formation of the polymer layers increased the electrode surface as a result of enhanced layer of gold nanoparticles electrodeposited on the electrode

surface [27]. Table S-1 (in Supplementary material) presents the results of the present study obtained for the electrode with electrodeposited gold nanoparticles in the absence and presence of a polymer support. Clearly, the presence of the polymer support led to the better activity of the modified electrode.

3.2. Electrodeposition of gold nanoparticles on the surface of the polymer support

The influence of the scan rate for the gold nanoparticle electrodeposition on the surface of the polymer coated electrode was investigated. For this purpose, the polymer coated electrode was placed in 3.0 mmol L^{-1} gold(III) chloride containing 0.1 mol L^{-1} potassium nitrate with a potential in the range of –0.50 to +1.50 V at the different scan rates of 1, 2, 5, 7, 10, and 15 mV s^{-1}. The excess gold ions trapped on the electrode surface were removed in the potential range of –0.50 to +1.50 V at a scan rate of 50 mV s^{-1} in 10 CVs in 0.1 mol L^{-1} potassium nitrate. The current of this electrode with a layer of gold nanoparticles on the surface was investigated in a solution of 0.5 mol L^{-1} H_2SO_4. Based on the results obtained (Fig. 1B), a scan rate of 2 mV s^{-1} was selected as the optimum rate. At this scan rate, an adequately large layer of the gold nanoparticles was formed at the surface of the polymer film to create the maximum current.

The morphology of the PGE before modification and during modification was also investigated using FE-SEM. Fig. 2A shows the surface morphology of the unmodified PGE, whereas Fig. 2B shows the pretreated PGE. As shown here, the surface of the pretreated PGE has more porosity after the treatment, using cycling voltammery. Fig. 2C and Fig. 2D show the SEM images of PGE modified with the polymer film and the PGE modified with gold nanoparticles decorated on the polymer film. Clearly, a good dispersion of the gold nanoparticles with average size less than 100 nm (with the Gaussian distribution) was achieved on the surface of the electrode.

3.3. Optimization of single-stranded DNA concentration for the fabrication of the DNA biosensor

The electrode prepared in Section 3.2 was immersed in 20 μL of the ssDNA solutions of different concentrations at 3–4 ºC for 30 min. In this experiment, DNA aptamer was immobilized on the surface of the electrode. The electrode was then gently rinsed with DI water to remove any unbounded ssDNA at the electrode surface. The difference between the currents of the probe solution (after coating the electrode with gold nanoparticles and after immobilizing ss-DNA on the electrode) in the potential range of 0.00 to 0.40 V at a scan rate of 50 mV s^{-1} was considered as a signal. Immobilization of ssDNA at the electrode surface formed a resistant layer at the electrode surface and, therefore, decreased the electrode current (in the probe solution). Result (Fig. 3A) indicated that 15 μmol L^{-1} ssDNA yielded a better response (maximum current difference). The ssDNA immobilization remained constant with increasing the ssDNA concentration.

"Here Fig. 3"

3.4. Optimization of ssDNA immobilization time

Immobilization of ssDNA on the surface of the modified gold electrode was investigated over different durations. For this purpose, the modified gold electrode was placed into 20 μL of 15.0 μmol L^{-1} single-stranded DNA at 3 – 4 ºC for various time periods. Then, the biosensor was rinsed with water to remove any unbounded ssDNA before placing it in a solution of 1.0 mmol L^{-1} $K_3Fe(CN)_6/K_4Fe(CN)_6$ (in 0.10 mol L^{-1} KCl). Differences between the electrode currents (after coating with gold nanoparticles and after immobilization of ssDNA) were measured in the potential range of 0.00–0.40 V at a scan rate of 50 mV s^{-1}. The results (Fig. 3B) showed that 90 min was the optimum

time (with a maximum current difference) for the immobilization of DNA on the electrode surface. The amount of immobilized DNA did not change with increasing time and the signal was leveled off.

3.5. Optimization of pH and ion concentration for ss DNA-insulin interaction

Because electrochemical impedance spectroscopy is used as an analytical signal, it can be exploited to optimize the parameters involved in biosensor signal. Once the ssDNA immobilization on the electrode surface had been optimized, the parameters involved in the insulin detection of the biosensor were investigated for optimization. For this purpose, 1.0 mmol L^{-1} $K_3Fe(CN)_6/K_4Fe(CN)_6$ (in 0.10 mol L^{-1} KCl) was used as the probe solution. The charge transfer resistance of the solution was determined using the electrochemical impedance spectroscopy at a constant potential of 0.20 V with an initial frequency of 100 kHz, a final frequency of 0.05 Hz, and an amplitude of 0.01 V.

The influence of solution pH on the biosensor signal was studied in a 0.70 µmol L^{-1} insulin solution at different pH levels (4.0, 5.0, 5.3, 6.0, 7.0, 7.4, and 8.0) and in 5.0 mmol L^{-1} of $MgCl_2$ over 60 min at 25 ^{o}C. As already stated, the ssDNA on the surface of the biosensor makes a G-quadruplex structure with insulin. The charge transfer resistance of the biosensor in the probe solution was measured before and after the interaction. The difference between the two charge transfer resistances was reported as a signal (Table S-2, Supplementary material).

The charge transfer resistance of the biosensor after interaction with insulin increased because of the G-quadruplex formed. Based on the results obtained, pH 7.4 (phosphate buffer) was selected as the optimum pH level because the insulin-Gquadruplex interaction took place at this pH [28].

Ion has an essential effect on the formation of a G-quadruplex structure by stabilizing the G-quarter structure of the aptamer [28]. DNA has two negative charges per unit length, giving rise to a strong electrostatic interaction with metal ions [29]. For this purpose, $MgCl_2$ was added at different concentrations (5.0, 10.0, 15.0, and 20.0 mmol L^{-1}) to a solution of 0.7 µmol L^{-1} insulin at pH 7.4. Study has shown that this ion can interact with the carboxyl group of the target material to enhance the aptamer-target binding [28]. Thus, the aptasensor was placed in this solution at 25 ºC for 60 min before it was rinsed with DI water and placed in the probe solution. The difference between the charge transfer resistances of the two solutions (aptasensor after and before interaction with insulin) in the probe solution was reported as the response. Results shown in Fig. 4A confirm that Mg^{2+} at a concentration of 10 mmol L^{-1} had the greatest effect on forming the G-quadruplex structure. At higher Mg^{2+} concentrations, the electrostatic repulsion between the ions prevented the formation of G-quadruplex.

"Here Fig. 4"

3.6. Optimization of time and temperature for the ssDNA-insulin interaction

Time and temperature are the main factors affecting the interaction of insulin with the aptaensor. Hence, the biosensor was treated with 0.7 µmol L^{-1} insulin at pH 7.4 in the presence of 10 mmol L^{-1} $MgCl_2$ at different temperatures (10, 20, 25, 30, and 37 ºC) for 60 min. Then, the charge transfer resistance of the biosensor was measured in the probe solution as described above to determine the difference between the charge transfer resistances before and after interaction with insulin. Results are presented in Fig. 4B, indicating that a temperature of 20 ºC provided better conditions for the insulin–aptasensor interaction [29**].**

To study the effect of interaction time, the aptasensor was placed in a 0.7 µmol L^{-1} insulin solution at pH 7.4 in the presence of 10 mmol L^{-1} $MgCl_2$ over different time

periods. The charge transfer resistance of the biosensor was measured in the probe solution as described above. The results (Fig. 5) indicated that 90 min was the best time period for the interaction of insulin with the aptasensor.

"Here Fig. 5"

4. Figures of merit

The linear dynamic range, limit of detection, reproducibility, and stability of the aptasensor for the determination of insulin were studied. The biosensor was used to measure different concentrations of insulin under the optimum conditions. Fig. 6 presents the Nyquist plots of the biosensor after its interaction with various concentrations of insulin with the regression equation of $\Delta R_{ct} = 0.1327C_{Ins} + 1.1103$ ($R^2 = 0.9944$) for insulin concentrations of 1.0 − 1000 nmol L^{-1}. The estimated limit of detection (LOD) was 0.27 nmol L^{-1} insulin based on LOD = $3S_{bk}/m$. "**Here Fig. 6"**

To investigate the repeatability and reproducibility of the proposed biosensor as its two important factors, the relative standard deviation of the responses of five sample biosensors wers measured for 100 nmol L^{-1} insulin to obtain an RSD value of 5.1% for the five aptasensors under identical conditions. Moreover, the repeatability of the sensor was studied using the aptamer with a solution containing 100 nmol L^{-1} insulin. The obtained RSD value of 3.1% for the five replicate determination under identical conditions.

To investigate the stability of the biosensor, different biosensors were prepared separately under similar conditions and stored at 4 °C for 10 days. The charge transfer resistance of each biosensor was measured in the probe solution at two-day intervals. No differences were observed in their R_{ct} values after 8 days. After this period, however, R_{ct} began to decrease slowly so that it declined to only 93.7% of the original R_{ct} after 10 days.

5. Method selectivity and real sample analysis

The selectivity of the aptasensor was checked with 500-fold excess concentration of several potential interfering substance, in the presence of 50 nmol L^{-1} insulin. The results showed that glycerine, *o*-cresol, urea, L-cysteine, phenylalanine, glucose, uric acid, glycine, HCO_3^-, and SO_4^{2-} have not affect the selectivity. However, more than 50-fold of Bovine serum albumin, Luteinizing hormone, and Follicle stimulating hormone interfere with the insulin determination.

The applicability of the biosensor for the analysis of insulin was investigated in real urine and plasma samples as complex matrices. The plasma sample was filtrated and stored in the refrigerator after collection. It was subsequently diluted to a 1:1 ratio with the phosphate buffer solution and adjusted to pH 7.4 before the protein content was separated. The insulin content in the plasma sample was analyzed with the biosensor using the standard addition method. Additionally, a plasma sample was mixed in another experiment with 10% (w/v) trichloroacetic acid (TCA) and centrifuged for 10 min at 4000 rpm before it was filtrated. The resulting solution was diluted two times with the phosphate buffer solution (pH 7.4) and analyzed with the aptasensor using the standard addition method. The results are reported in Table 1. Clearly, the presence of proteins in plasma did not interfere with insulin detection and determination.

Immediately after collection, one urine sample was centrifuged and filtrated before storage in the refrigerator. This sample was diluted 2 times with the phosphate buffer solution (pH 7.4). The insulin content was measured with the biosensor using the standard addition method. The results are reported in Table 1. "**Here Table 1"**

6. Conclusion

In this study, an aptasensor was successfully fabricated and used for the extraction and determination of insulin in a complex matrix. Insulin was analyzed using the

electrochemical impedance spectroscopy method. In this biosensor, poly-orthophenylene was used in the form of a film coating via the electropolymerization process. This polymer layer increases the immobilization sites for the DNA after electrodeposition of gold nanoparticles. The figures of merit of the biosensor were compared with those reported elsewhere for recently reported electrochemical methods [30-40] (Table 2). The proposed method was found to yield a better limit of detection for insulin determination. Comparison of the new biosensor with those reported in previous studies indicated that the biosensor had a low detection limit and a wide linear dynamic range for insulin analysis. Real sample analysis revealed that the proposed aptasensor could be successfully used as a specific and sensitive tool for the detection and determination of plasma insulin in the presence of proteins.

"**Here Table 2"**

Acknowledgments

The authors wish to thanks to the Centre of Excellence in Sensor and Green Chemistry for supporting this work.

References

[1] Ali A. Ensafi, P. Nasr-Esfahani, E. Heydari-Bafrooei, B. Rezaei, Redox targeting of DNA anchored to MWCNTs and TiO_2 nanoparticles dispersed in poly dialyldimethylammonium chloride and chitosan, Colloids and Surfaces B: Biointerfaces 121 (2014) 99–105.

[2] N. Farkhari, S. Abbasian, A. Moshaii, M. Nikkhah, Mechanism of adsorption of single and double stranded DNA on gold and silver nanoparticles: Investigating some important parameters in bio-sensing applications, Colloids and Surfaces B: Biointerfaces 148 (2016) 657-664.

[3] C.L.A. Hamula, J.W. Guthrie, H. Zhang, X. F. Li, X. C. Le, Selection and analytical applications of aptamers, TrAC, Trends Anal. Chem. 25 (2006) 681-691.

[4] Y. Li, Q. Wang, Y. Zhang, D. Deng, H. He, L. Luo, Z. Wang, A label-free electrochemical aptasensor based on graphene oxide/double-stranded DNA nanocomposite, Colloids and Surfaces B: Biointerfaces, 145 (2016) 160-166.

[5] J.O. Lee, H.M. So, E.K. Jeon, H. Chang, K. Won, Y. H. Kim, Aptamers as molecular recognition elements for electrical nanobiosensors, Anal. Bioanal. Chem. 390 (2008) 1023-1032.

[6] Ali A. Ensafi, N. Kazemifard, B. Rezaei, A Simple and sensitive fluorimetric aptasensor for the ultrasensitive detection of arsenic(III) based on cysteamine stabilized CdTe/ZnS quantum dots aggregation, Biosens. Bioelectronics 7 (2016) 499-505.

[7] B. Madru, F. Chapuis-Hugon, V. Pichon, Novel extraction supports based on immobilised aptamers: Evaluation for the selective extraction of cocaine, Talanta 85 (2011) 616-624.

[8] C. Forier, E. Boschetti, M. Ouhammouch, A. Cibiel, F. cDucongé, M. Nogré, M. Tellier, D. Bataille, N. Bihoreau, P. Santambien, S. Chtourou, G. Perret, DNA aptamer

affinity ligands for highly selective purification of human plasma-related proteins from multiple sources, J. Chromatogr A 1489 (2017) 39-50.

[9] L. Qiao, B. Lv, X. Feng, C. Li, A new application of aptamer: One-step purification and immobilization of enzyme from cell lysates for biocatalysis, J. Biotech. 203 (2015) 68-76.

[10] B. Madru, F. Chapuis-Hugon, V. Pichon, Novel extraction supports based on immobilised aptamers: evaluation for the selective extraction of cocaine. Talanta 85 (2011) 616-622.

[11] H. Ulrich, C. Wrenger, Disease-specific biomarker discovery by aptamers. Cytometry. Part A: J. Intern. Soc. Anal. Cytol. 75 (2009) 727-729.

[12] M. Mascini, I. Palchetti, S. Tombelli, Nucleic acid and peptide aptamers: fundamentals and bioanalytical aspects, Angew. Chem. Int. Ed. 51 (2012) 1316–1332.

[13] M.O. Yanik1, E.A. Yigit, Y.E. Akansu, E. Sahmetlioglu, Magnetic conductive polymer-graphene nanocomposites based supercapacitors for energy storage, in press, doi.org/10.1016/j.energy.2017.07.022.

[14] D. Choi, M. Lee, H. Kim, W. Chu, D. Chun, S.-H. Ahn, C.S. Lee, Fabrication of transparent conductive tri-composite film for electrochromic application, Applied Surface Sci**.** in press, doi.org/10.1016/j.apsusc.2017.07.076.

[15] D. Liu, Y. Zhao, R. Tan, L.-L. Tian, Y. Liu, H. Chen, F. Pan, Novel conductive binder for high-performance silicon anodes in lithium ion batteries, Nano Energy, 36 (2017) 206-212.

[16] E. Bayram, E. Akyilmaz , Development of a new microbial biosensor based on conductive polymer/multiwalled carbon nanotube and its application to paracetamol determination, Sens. Actuators B 233 (2016) 409-418.

[17] Ali A. Ensafi, M. Amini, B. Rezaei**,** Biosensor based on ds-DNA decorated chitosan

modified multiwall carbon nanotubes for voltammetric biodetection of herbicide amitrol, Colloids and Surfaces B: Biointerfaces 109 (2013) 45–51.

[18] Z.B. Anna, B. Patrycja, J. Petr, E. Petrovský, B. Pavel, H. Daniel, Magnetoconductive maghemite core/polyaniline shell nanoparticles: Physico-chemical and biological assessment, Colloids and Surfaces B: Biointerfaces 141 (2016) 382–389.

[19] T. Yang, H. Chen, R. Yang, X. Wang, F. Nan, K. Jiao. The effect of material composition of 3-dimensional graphene oxide and self-doped polyaniline nanocomposites on DNA analytical sensitivity, Colloids and Surfaces B: Biointerfaces 133 (2015) 24–31.

[20] M. Cui, Z. Song, Y. Wu, B. Guo, X. Fan, X. Lou, A highly sensitive biosensor for tumor maker alpha fetoprotein based on poly(ethylene glycol) doped conducting polymer PEDOT, Biosens Bioelectron 79 (2016) 736-741.

[21] B. Rezaei, M.K. Boroujeni, A.A. Ensafi, Development of sudan II Sensor based on modified treated pencil graphite electrode with DNA, *o*-phenylenediamine, and gold nanoparticle bioimprinted polymer, Sens. Actuators B 222 (2016) 849-856.

[22] K. Sao, H.Q. Cao, Q. Qiu, Selective intercalation of *o*-phenylene diamine into molybdenum oxide layers, Materials Res. Bulletin 44 (2009) 678-681.

[23] E. Ferrannini, A. Mari, Beta cell function and its relation to insulin action in humans: a critical appraisal, Diabetologia 47 (2004) 943-956.

[24] Ali A. Ensafi, Elaheh Khoddami, B. Rezaei, Mehdi Jafari-Asl, A supported liquid membrane for microextraction of insulin, and its determination with a pencil graphite electrode modified with RuO_2-graphene oxide, Microchim. Acta 182 (2015) 1599–1607.

[25] A. Verdian-Doghaei, M.R. Housaindokht, Spectroscopic study of the interaction of insulin and its aptamer–sensitive optical detection of insulin, J. Luminescence 159 (2015) 1–8.

[26] A. Ozcan, Y. Şahin, Preparation of selective and sensitive electrochemically treated

pencil graphite electrodes for the determination of uric acid in urine and blood serum, Biosens. Bioelectron. 25 (2010) 2497-2502.

[27] T. An, W. Choi, E. Lee, S.J. Cho, G. Lim, Fabrication of conducting polymer micro/nanostructures coated with Au nanoparticles for electrochemical sensors, J. Nanosci. Nanotechnol. 12(6) (2012) 4975-4978.

[28] C. M. Timmer, N. L. Michmerhuizen, A. B. Witte, M. V. Winkle, D. Zhou, K. Sinniah, An isothermal titration and differential scanning calorimetry study of the G-quadruplex DNA−insulin interaction, J. Phys. Chem. B 118 (2014) 1784-1790.

[29] W.O. Tucker, K.T. Shum, J.A. Tanner, G-quadruplex DNA aptamers and their ligands: structure, function and application, Curr. Pharm. Design 18 (2012) 2014-2026.

[30] S. Viswanathan, J. Ho, Dual electrochemical determination of glucose and insulin using enzyme and ferrocene microcapsules, Biosens. Bioelectron. 22 (2007) 1147–1153.

[31] A. Kaur, N. Verma, Electrochemical biosensor for monitoring insulin in normal individuals and diabetic mellitus patients, Eur. J. Exp. Biol. 2 (2012) 389–395.

[32] V. Serafín, L. Agüí, P. Yáñez-Sedeño, J.M. Pingarrón, Electrochemical immunosensor for the determination of insulin-like growth factor-1 using electrodes modified with carbon nanotubes–poly (pyrrole propionic acid), Biosens. Bioelectron. 52 (2014) 98–104.

[33] E. Martínez-Periñán. M. Revenga-Parra. M. Gennari. F. Pariente. R. Mas-Ballesté. F. Zamora. E. Lorenzo, Insulin sensor based on nanoparticle-decorated multiwalled carbon nanotubes modified electrodes, Sens. Actuators B 222 (2016) 331-338.

[34] W. Gorski, C.A. Aspinwal, J.R.T. Lakey, R.T. Kennedy, Ruthenium catalyst for amperometric determination of insulin at physiological pH, J. Electroanal. Chem. 425 (1997) 191-199.

[35] J.Y. Gerasimov, C.S. Schaefer, W. Yang, R.L. Grout, R.Y. Lai, Development of an

electrochemical insulin sensor based on the insulin-linked polymorphicregion, Biosens. Bioelectronics 42 (2013) 62-68.

[36] Y. Yu, M. Guo, M. Yuan, W. Liu, J. Hu, Nickel nanoparticle-modified electrode for ultra-sensitive electrochemical detection of insulin, Biosens. Bioelectronics 77 (2016) 215-219.

[37] E. Habibi, E. Omidinia, H. Heidari, M. Fazli,, Flow injection amperometric detection of insulin at cobalt hydroxide nanoparticles modified carbon ceramic electrode, Anal. Biochem. 495 (2016) 37-41.

[38] R.M. Snider, M. Ciobanu, A.E. Rue, D.E. Cliffel, A multiwalled carbon nanotube/dihydropyran composite film electrode for insulin detection in a microphysiometer chamber, Anal. Chim. Acta 609 (2008) 44-52.

[39] M. Jafari-Asl, E. Shams, M.K. Amini, Silica gel modified carbon paste electrode for electrochemical detection of insulin, Electrochim. Acta 56 (2011) 4390-95.

[40] B. Rafiee, A.R. Fakhari, Electrocatalytic oxidation and determination of insulin at nickel oxide nanoparticles-multiwalled carbon nanotube modified screen printed electrode, Biosens. Bioelectron. 460 (2013) 130-135.

Figures Caption:

Fig. 1. A) Survey of steps for the biosensor preparation in the probe solution, a): Bare PGE, b): Activated PGE, c): The polymer-film-activated PGE, d): Au-modified polymer-film-activated PGE, e): DNA-Au- polymer-film-activated PGE; **B)** Survey of the effect of the scan rate for gold nanoparticles electrodeposition (in 3.0 mmol L^{-1} gold(III) chloride and 0.1 mol L^{-1} KNO_3) on the surface of the coated polymer-PGE in a solution containing 0.5 mol L^{-1} H_2SO_4 with 2, 1, 5, 7, 10, 15 mV s^{-1} (n=3).

Fig. 2. FE-SEM images of A): Bare PGE B): Pretreated PGE; C): Polymer film modified PGE; and D): Au@polymer film modified PGE (with the Gaussian distribution of the Au nanoparticles).

Fig. 3. A) Survey of the effect of ssDNA concentration (3.0, 7.0, 10.0, 15.0, 20.0 µmol L^{-1}) for fabrication ss DNA biosensor in temperature 3-4 ^oC for 30 min in probe solution (n=3); **B)** Survey of the effect of immobilization time (30, 60, 90, 120) for fabrication 15.0 mmol L^{-1} ss DNA biosensor in temperature 3-4 ^oC.

Fig. 4. A) Effect of the salt ($MgCl_2$) concentration (5.0, 10.0, 15.0, 20.0 mmol L^{-1}) for G-quadruplex structure formation after interaction of the biosensor with 0.7 µmol L^{-1} insulin at pH 7.4 (PBS solution) and at 25 ^oC for 60 min; **B)** Effect of temperature (10, 20, 25, 30, 37 ^oC) for the G-quadruplex structure formation after interaction of the biosensor with 0.7 µmol L^{-1} insulin at pH 7.4 (PBS solution) in 10.0 mmol L^{-1} $MgCl_2$ and at 25^oC for 60 min.

Fig. 5. Influence of time (30, 60, 90, 120 min) for the G-quadruplex structure formation with 0.7 µmol L^{-1} insulin at pH 7.4 (PBS solution in the presence of 10.0 mmol L^{-1} $MgCl_2$, at 20 ^oC.

Fig. 6. Calibration curve for the biosensor in the probe solution in the presence of the different concentration of insulin: 1.0, 50.0, 300, 600,800, 1000 nmol L^{-1}; Nyquist plots of aptasensor in various concentration of insulin. Conditions: pH 7.4 (PBS solution in the presence of 10.0 mmol L^{-1} $MgCl_2$) at 20^{o}C for 90 min.

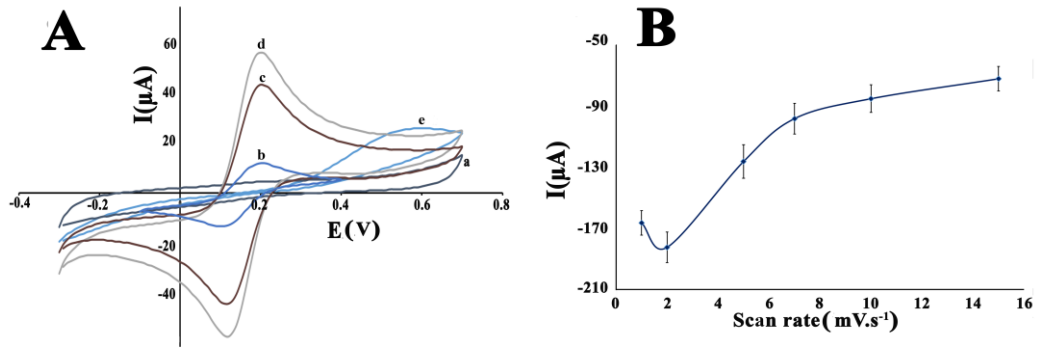

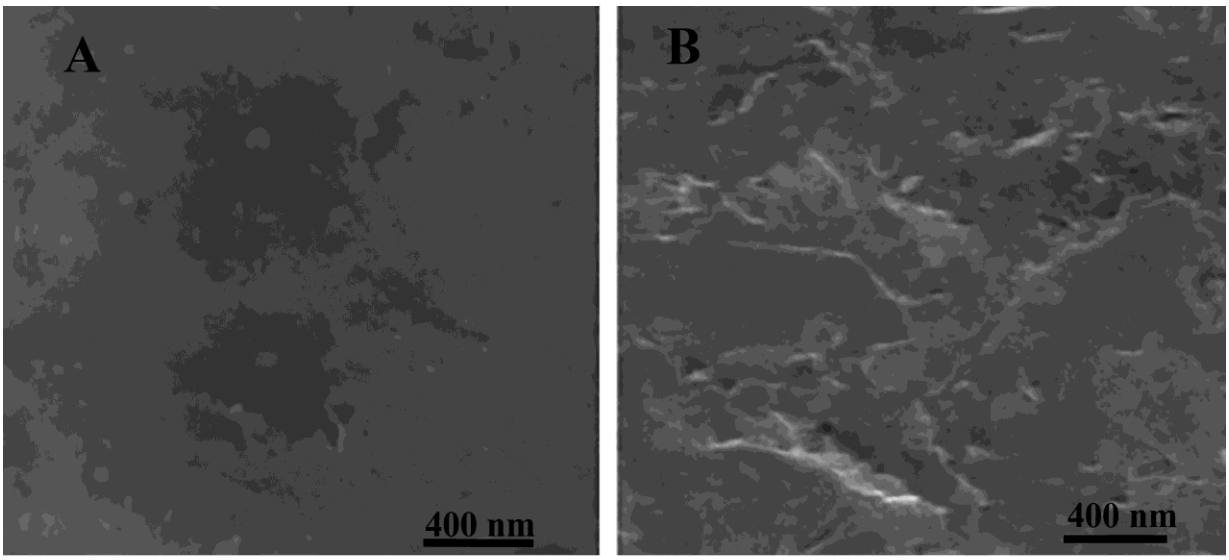

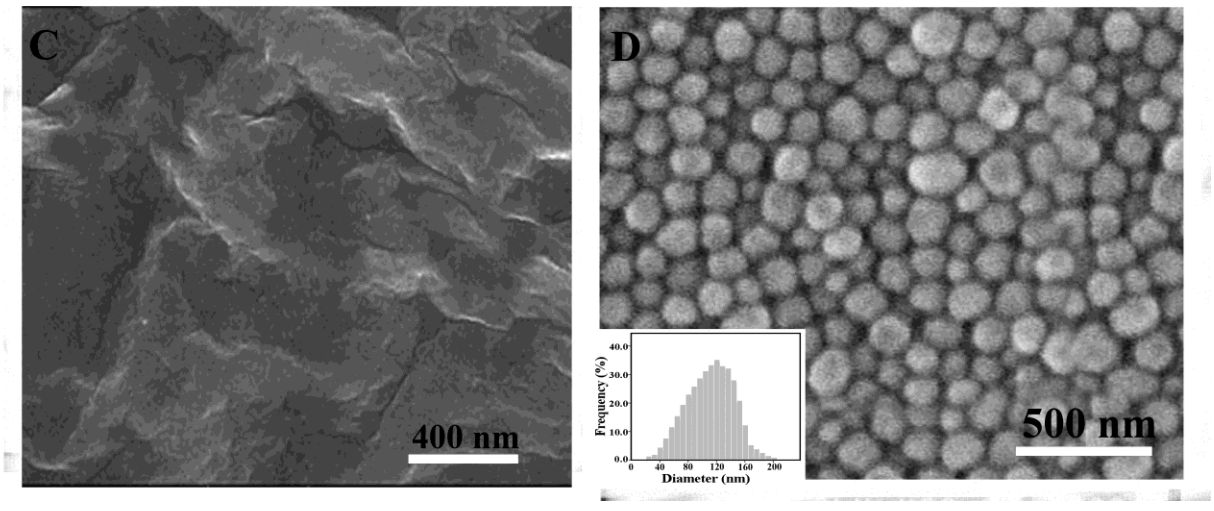

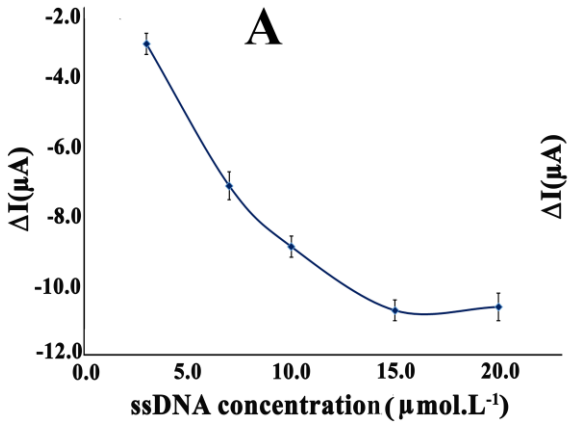

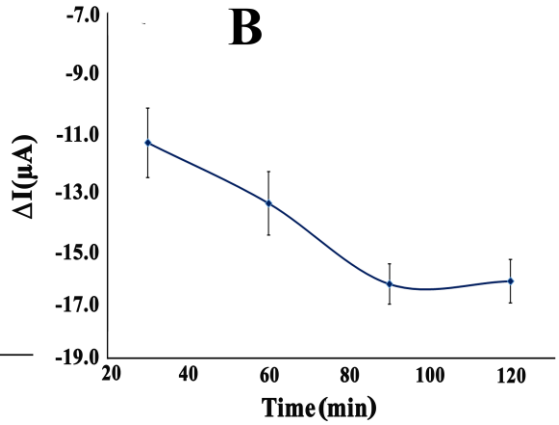

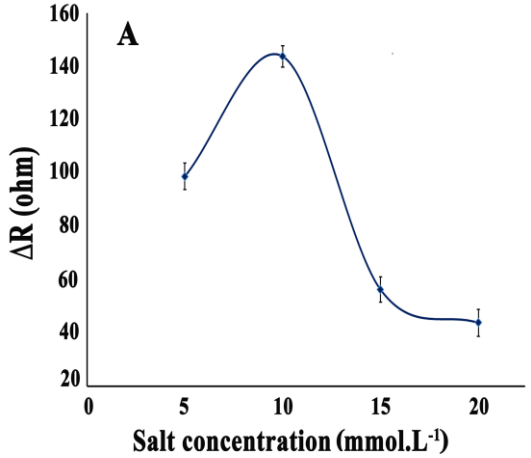

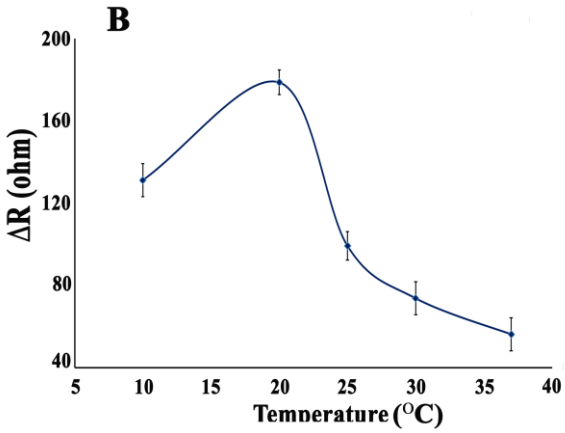

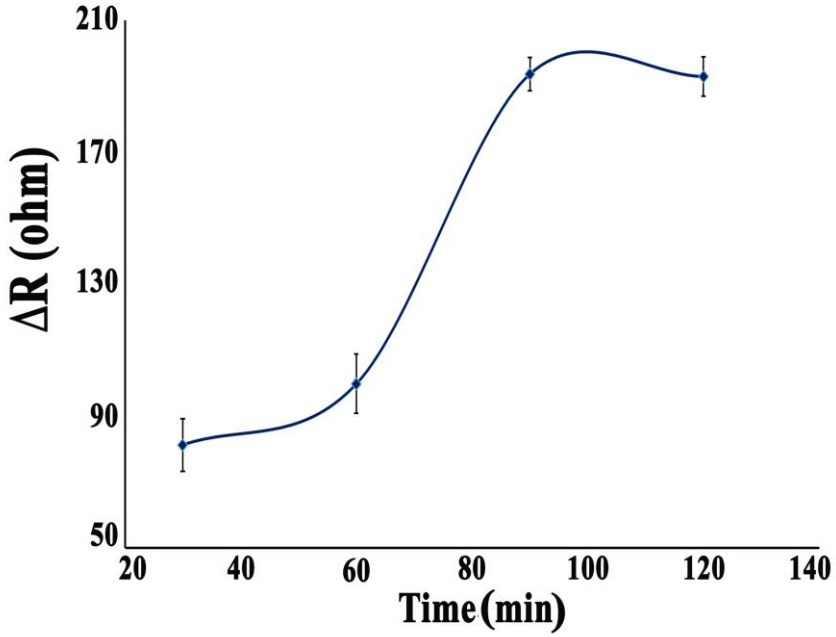

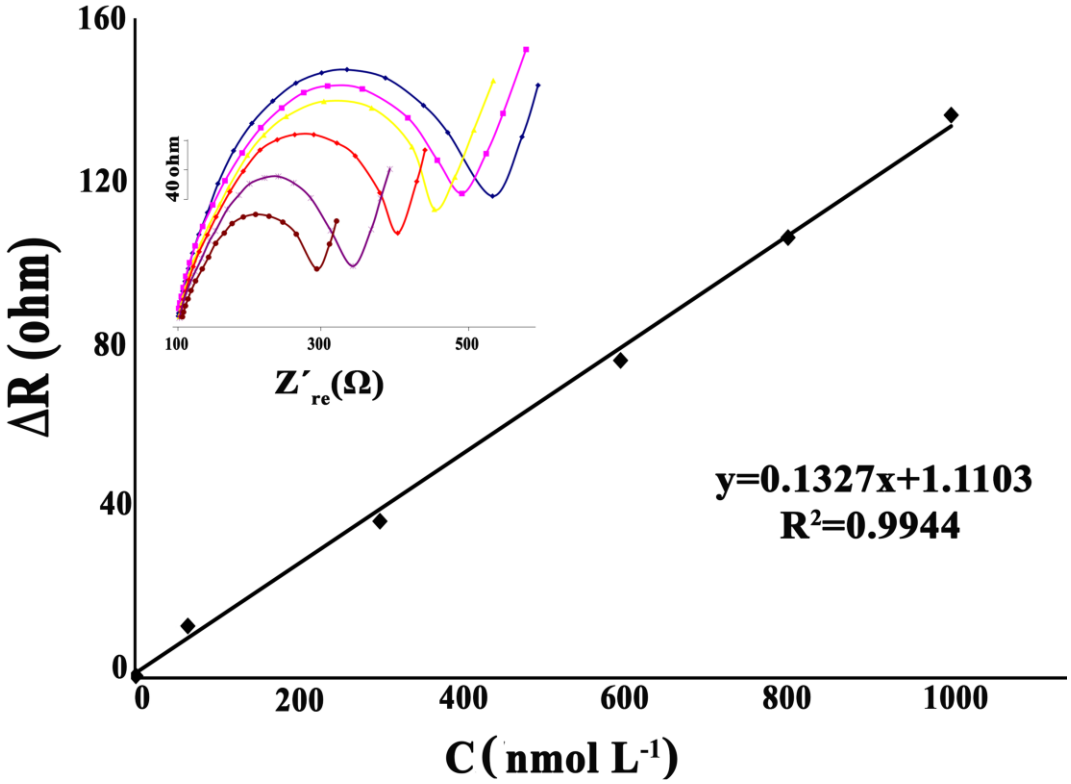

Table 1. Real sample analysis.

Sample	Spiked insulin/nmol L^{-1}	Found insulin/nmol L^{-1}	Recovery/%
Plasma*	-	0.055±0.005	-
Plasma**	50.0	51.5±0.5	103.0
Plasma***	70.0	62.2 ±0.2	88.9
Urine	50.0	47.0±1.0	94.0
Urine	100.0	93.0±3.0	93.0

*Plasma sample without spiked insulin.

**Plasma sample before pretreatment with TCA.

*** Plasma sample after pretreatment with TCA.

Table 2. Comparison of the proposed method with several electrochemical methods for the detection of insulin**.**

Method	Limit of detection	Linear dynamic range	Ref.
Pt/anti-insulin antibody immunosensor	0.07 nmol L^{-1}	0.17–170 nmol L^{-1}	30
CPE with red blood cells	0.006 μmol L^{-1}	0.006–0.09 μmol L^{-1}	31
GCE/MWCNTs/ poly(pyrolepropionic acid)	0.2 nmol L^{-1}	0.5–1000 μmol L^{-1}	32
$Ni(OH)_2$/Nafion-MWCNTs	85 nmol L^{-1}	0.1–10 μmol L^{-1}	33
RuOx-carbon fiber	23.0 nmol L^{-1}	0.10 –1.00 μmol L^{-1}	34
Carbon microelectrode RuO/RuCN	10 nmol L^{-1}	10 –200 nmol L^{-1}	35
NiNPs-indium tin oxide	0.1 nmol L^{-1}	1–125 nmol L^{-1}	36
$Co(OH)_2$/carbon ceramic electrode	0.11 nmol L^{-1}	Not reported	37
MWCNTs-dihydropyran composite	1.0 μmol L^{-1}	0.8–2.5 mol L^{-1}	38
Silica gel	36 pmol L^{-1}	90-400 pmol L^{-1}	39
NiO-MWCNTs	6.1 nmol L^{-1}	20.0- 260 nmol L^{-1}	40
This work	0.027 nmol L^{-1}	1.0–1000 nmol L^{-1}	-